

# A Switched Z-Source and Switched Capacitor Multi-Level Inverter Integrated Low Voltage Renewable Source for Grid Connected Application

Sapavath Sreenu<sup>1</sup>, Dr. J Upendar<sup>2</sup>

<sup>1</sup>Department of Electrical Engg., University College of Engineering, Osmania University Hyderabad, India; sreenu06274@gmail.com

<sup>2</sup>Department of Electrical Engg., University College of Engineering, Osmania University Hyderabad, India; dr.8500003210@gmail.com

\*Correspondence: Sapavath Sreenu; sreenu06274@gmail.com

**ABSTRACT-** Most of the renewable sources generate power at lower voltage levels in the range of 20-50V which cannot be utilized by the loads. Therefore, stacking multiple modules in series increases the voltage level or using conventional boost converter or QZS is helpful. However, due to series stacking and boost converter or QZS there is a great power loss and also have reliability issues. The QZS inverter has very less boosting gain in the range of 2 times. The conventional boost converter or QZS is replaced with SZSC for voltage boosting and inverter operation. The SZSC boosts the voltage 4-5 times to the input voltage level. For further mitigation of harmonics, the conventional 6-switch inverter is replaced with switched capacitor MLI. Multiple renewable sources are at the input which include PV array, battery unit and PMSG wind module. The battery unit is a support to the renewable sources PV array and wind module. The DC link voltage stability is achieved by the battery unit placed in parallel to the renewable sources. The renewable sources share power to the grid through the SZSC and switched capacitor MLI. For DC voltage stability a CV control is integrated to SZSC. And for synchronized power sharing to the grid, a grid voltage feedback synchronization control is included for the control of MLI. A low rating renewable system is modelled and integrated to grid using Simulink MATLAB software. A comparative analysis is carried out operating the system with QZS and SZSC. The performances of the SZSC and MLI are evaluated by the graphs generated by the simulation of the modelled system.

**Keywords:** QZS (Quasi Z-Source), SZSC (Switched Z-Source Converter), MLI (Multi-Level Inverter), PV (Photo Voltaic), PMSG (Permanent Magnet Synchronous Generator), CV (Constant Voltage).

## ARTICLE INFORMATION

**Author(s):** Sapavath Sreenu<sup>1</sup>, Dr. J Upendar;

**Received:** 16/02/2024; **Accepted:** 19/04/2024; **Published:** 05/05/2024;

**E- ISSN:** 2347-470X;

**Paper Id:** IJEER 1602-12;

**Citation:** 10.37391/IJEER.120218

**Webpage-link:**

<https://ijeer.forexjournal.co.in/archive/volume-12/ijeer-120218.html>



**Publisher's Note:** FOREX Publication stays neutral with regard to Jurisdictional claims in Published maps and institutional affiliations.

## 1. INTRODUCTION

Due to utilization of fossil fuel technology for generation of electric power is leading to disasters in environment. Fossil fuel power generation has to be replaced with renewable power which generates electricity using natural resources like solar irradiation, wind speeds, tidal energy etc. It is a greater challenge to integrate renewable energy sources to the grid as these sources are unpredictable, unreliable and always vary with respect to the available natural sources. There is also a drawback of low voltage levels created by the renewable Sources. In order to increase the voltage levels multiple power electronic devices, have to be used which introduce power loss and switching losses. The low voltage levels are

generally created by renewable sources like PV plants, fuel cells, battery and super capacitor units etc [1]. In order to increase the voltage levels conventional boost converter topologies are used which have very less efficiency and higher ripple. In order to have higher gains of voltage boosting high gain dc dc converters are used which operates only for low power rating system.

Traditional method of integrating Renewable Sources comprises of a conventional boost converter connected to 6-switch inverter [2]. The QZS increase the input voltage levels by 2 to 2.5 times which later on converted to AC by the 6-switch inverter. In this paper this traditional QZS is replaced with SZSC connected to the Renewable Sources [3]. The SZSC boosts the voltage of the renewable source with a high gain of 4 to 5 times. The high gain DC voltage is fed to a switched capacitor MLI converting it to multi-level AC voltage [4]. The multilevel AC voltage has lesser harmonics as compared to two level voltage generated by the 6-switch inverter. The SZSC has a single power electronic switch with variable duty ratio (D) determined by the required output voltage. The MLI operates in synchronization with the three-phase grid by taking feedback from the grid source. The structure of the proposed test system with Renewable Sources, SZSC and MLI can be observed in *figure 1*.

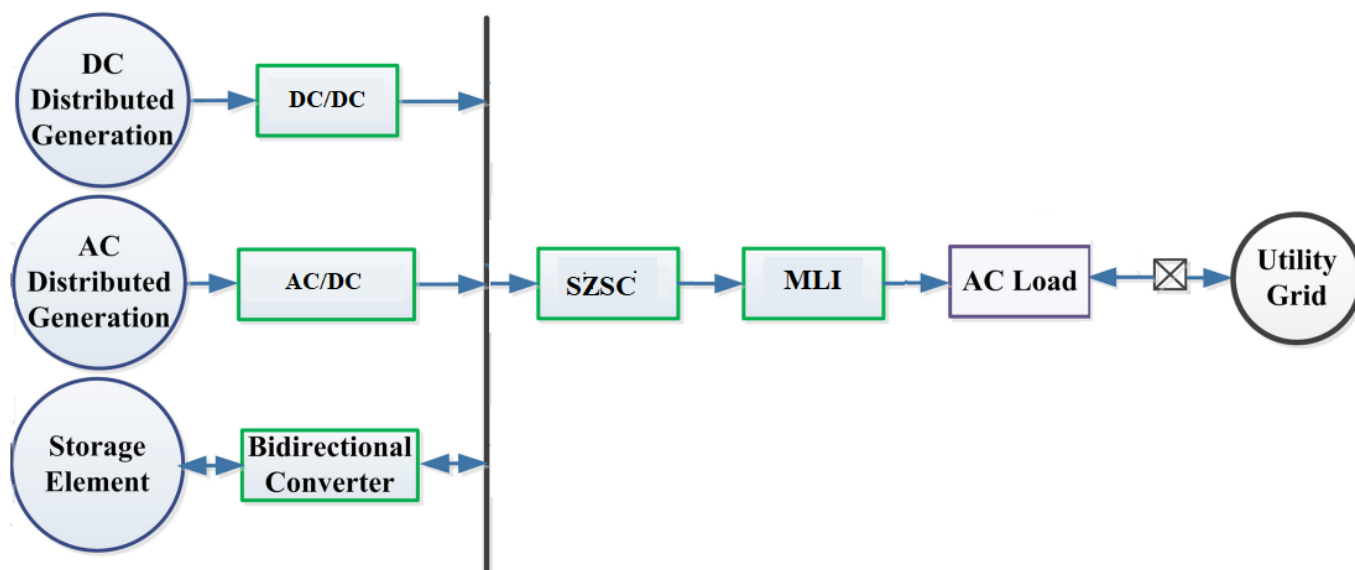


Figure 1: Proposed system structure with renewable sources, SZSC and MLI

As per figure 1 the DC distribution generation is the photovoltaic array and ac distribution generation PMSG wind farm. To support these two Renewable Sources a battery storage element is connected for DC link voltage stabilization [5] [6]. There will be an exchange of power between the storage element and the Renewable Sources as per the power generation. The common DC link is connected to SZSC which boosts the low DC link voltage to higher voltage. the DC high voltage generated by the SZSC is converted to AC by the switched capacitor MLI. An AC load is connected between the utility grid and the switched capacitor MLI [7]. The AC load consumes power either from the renewable module or the utility grid as per the availability of renewable power. The renewable power is injected to the utility grid either during low load demand or no-load condition. The required DC voltage at the output of SZSC is acquired by CV control with reference voltage set as per requirement. The switched capacitor MLI is controlled by level shifted multi carrier Sin PWM (Pulse Width Modulation) technique. The reference to the PWM is provided by synchronization voltage reference estimator with feedback from grid voltages.

This paper is organized with introduction to the proposed system structure included in section 1 followed by renewable sources modelling in section 2. The section 2 has the internal circuit structure modelling of renewable sources with specified operation and control. In section 3 the design of SZSC, switched capacitor MLI is configured and the operating principles are explained as per switching modes. The simulation modelling and results are discussed in section 4, where the graphs of different parameters are plotted and studied. The graphs are analysed for validating the performance of each module and its capability. A comparative analysis to conventional circuit structure is done determining

the quality of the proposed system. The final section 5 has the conclusion to the paper finalizing the result parameters and proposed design significance. The conclusion is followed by references of the topics covered in this paper.

## 2. RENEWABLE SOURCES MODELLING

As mentioned in introduction section the input to the SZSC is renewable sources connected with battery pack supporting the system. The renewable sources used are PV array and PMSG wind farm which generate power using solar irradiation and wind speed respectively [8].

For maximum power extraction from these renewable sources DC-DC converters are connected operated by maximum power point tracking (MPPT) algorithm. The PV array is connected to a boost converter and the wind farm is integrated with buck-boost converter. Both the boost and buck-boost converters are unidirectional converters which only extract power from the sources. Along with the PV array and wind farm, a battery pack is connected with bidirectional DC-DC converter [9].

This battery converter switches are controlled by CV control with reference DC link voltage ( $V_{dc\ ref}$ ). The proposed structure of the input source module can be seen in figure 2.

The MPPT controller takes feedback from PV panel voltage and current for estimation of the required duty ratio for maximum power extraction. The connection of multiple panels in parallel or series makes a PV array which is represented as a solar plant. This PV array connected to the booster converter controlled by the MPPT controller circuit structure is shown in figure 2.

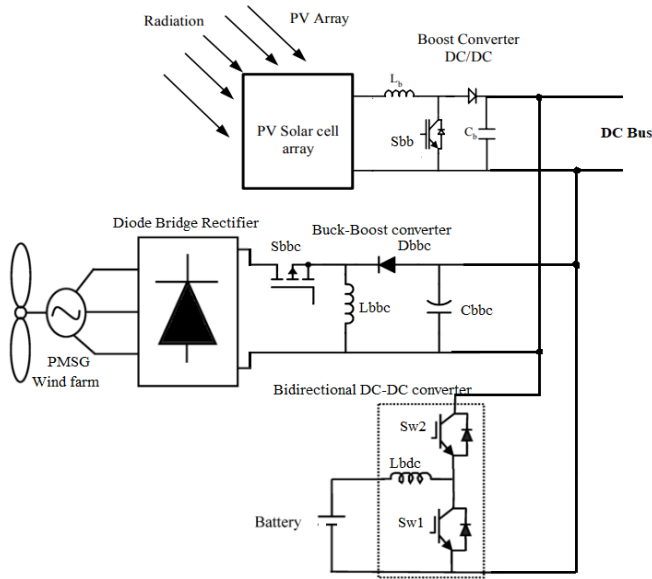


**Figure 2:** Input source module with renewable sources and battery unit

The boost converter switch ( $S_{bb}$ ) is controlled by P&O MPPT method by taking feedback from PV array voltage and current. The duty ratio of  $S_{bb}$  is varied as per the voltage and current ( $P_{pv}$  and  $I_{pv}$ ) change occurred in the PV array [10]. These values change as per the variation in solar irradiation. The update of new duty ratio ( $D_{new}(t)$ ) is expressed as:

$$D_{new}(t) = D(t - 1) + \Delta D \begin{cases} \text{If } P(t) > P(t - 1) \text{ and } V(t) > V(t - 1) \\ \text{If } P(t) < P(t - 1) \text{ and } V(t) < V(t - 1) \end{cases} \quad (1)$$

$$D_{new}(t) = D(t - 1) - \Delta D \begin{cases} \text{If } P(t) < P(t - 1) \text{ and } V(t) > V(t - 1) \\ \text{If } P(t) > P(t - 1) \text{ and } V(t) < V(t - 1) \end{cases} \quad (2)$$

In the given expressions (1) and (2) 'P(t) V(t)' represent and 'P(t-1)V(t-1)' are past PV array powers and voltages respectively.  $\Delta D$  is the update duty ratio value to the past duty ratio  $D(t-1)$ . The updated  $D_{new}(t)$  is compared to high frequency carrier sawtooth waveform generating pulse for the switch  $S_{bb}$ . As per the change in the  $D_{new}(t)$  maximum power is extracted from the PV array. The wind farm module has standalone generator (PMSG) driven by wind turbine propelled by wind flow.

The 3-ph uncertain voltage from PMSG are converted to unregulated DC with a diode bridge rectifier (DBR). The unregulated DC voltage is stabilized and maximum power extraction from PMSG is achieved by buck-boost converter. A buck-boost converter is adopted for voltage stability during high and low wind speeds. The wind farm converter switch is controlled by Power Signal Feedback (PSF) MPPT algorithm [11]. The PSF algorithm takes rotor speed ( $w_r$ ) as reference for

generation of required duty ratio of the switch  $S_{bbc}$ . The reference power ( $P_{ref}$ ) generated from the  $w_r$  variable is expressed as:

$$P_{ref} = K_{opt} \cdot w_r^3 \quad (3)$$

Here,  $K_{opt}$  is the optimal MPPT gain tuned as per the reference signal generation. From the  $P_{ref}$  signal generated, the duty ratio  $D_{b-b}(t)$  is generated as per given expression:

$$D_{b-b}(t) = (K_p + \int K_i \cdot dt) \left( \frac{P_{ref}}{w_r} \right) \quad (4)$$

The MPPT regulator is a PI controller with proportional and integral gains ( $K_p$  and  $K_i$ ) tuned as per the damping of  $D_{b-b}(t)$ . The buck-boost converter output terminals are connected in parallel to the boost converter of PV array for sharing power to the SZSC. As both the renewable sources are unpredictable, unreliable and unstable, a battery module need to be connected at the DC link. The connection of the battery module stabilizes the DC link voltage and also provide storage facility for the renewable power. During low renewable power generation conditions, the battery module provides stored power to the load. Therefore, for charging and discharging of the battery pack (as per the renewable power availability) a bidirectional converter is included in the battery module.

The BDC is included with two switches  $Sw1$  and  $Sw2$  which are boost and buck switch respectively. These switches are operated alternatively with a NOT gate connected to one of the switches. The  $L_{bdc}$  is the energy storage element which provides boosting voltage to the DC link. When the ON time of switch  $Sw1$  is higher than the  $Sw2$  the converter operates in boost mode which discharges the battery. This mode is activated when the load demand is higher than the renewable power generation. When the renewable power generation is greater than the load demand, the excess power needs to be stored in the battery module. During this mode the battery  $Sw2$  ON time is higher than  $Sw1$  making the BDC to operate in buck state where the battery is charged by the excess renewable power.

The switches of the bidirectional converter are controlled by CV control with DC link voltage reference ( $V_{dc \text{ ref}}$ ) [12]. The  $V_{dc \text{ ref}}$  is set as per the required input voltage magnitude for the SZSC. In figure 2 switches  $Sw1$  and  $Sw2$  operate alternatively by a NOT gate connected to  $Sw2$ . The pulse to the switch  $Sw1$  is generated by comparison of high frequency carrier sawtooth waveform to the duty ratio  $D_{bdc}$  generated by CV control expressed as:

$$D_{bdc} = (K_{pdc} + \int K_{idc} \cdot dt) (V_{dc \text{ ref}} - V_{dc \text{ meas}}) \quad (5)$$

All the modules are connected in parallel as input to the SZSC which further boosts the voltage to higher magnitudes for utilization by loads. The modeling of SZSC and MLI are configured in next section.

### 3. CONVERTERS DESIGN

#### 3.1 QZS configuration

The QZS converter is considered to be basic initial converter in the family of Z-source converter topologies. The QZS has two capacitors and inductors connected in 'Z' pattern for voltage boosting purpose. The circuit structure of 3-ph QZS inverter can be observed in figure 3.

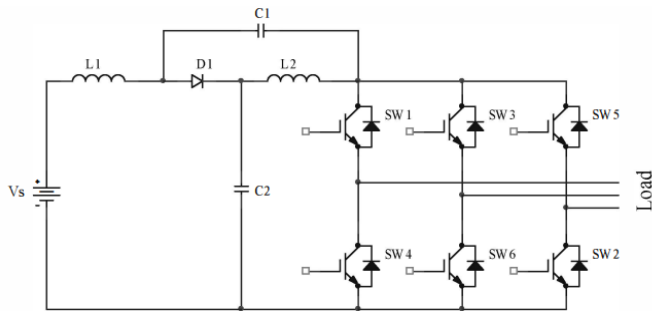


Figure 3: 3-Ph QZS inverter topology

The major limitation for the QZS converter is it can be integrated to only 6-switch voltage inverter circuit for shoot through mode. For voltage boosting the 6-switch inverter is operated in shoot through and non-shoot through modes. During the shoot through mode, any of the two switches in a leg of the 6-switch inverter are turned ON for small instant of time charging the inductors L1 L2. During non-shoot through mode the Sin PWM operates the inverter received with high voltage than the input voltage magnitude. The output voltage for the QZS converter is expressed as:

$$V_o = V_{in} (1/(1-2D)) \quad (6)$$

Considering the duty ratio (D) of the shoot through switches at 0.2 (20%) updated in equation (6), the gain is calculated as:

$$V_o = V_{in} \left( \frac{1}{1-2*0.2} \right) = 1.66 V_{in}$$

As per the mathematical equation the output voltage is 1.66 times of the input voltage. This gain can be maximum increased to 2 times with D set to 0.25 (25%).

Along with the limitation of 6-switch inverter integration (for shoot through) and low voltage gain (2times), the QZS also has very high voltage ripple content. This high ripple in the Vo creates harmonics on the AC side which leads to further damage to the load. Therefore, it is viable to upgrade the 3-ph QZS 6-switch inverter with a better converter topology to overcome these issues of power quality on both DC and AC sides.

#### 3.2 SZSC configuration

The proposed SZSC is a combination of conventional quasi-Z-source converter (QZSC) and a switching module [13]. The figure 4 illustrates the proposed SZSC with single switch and passive elements.

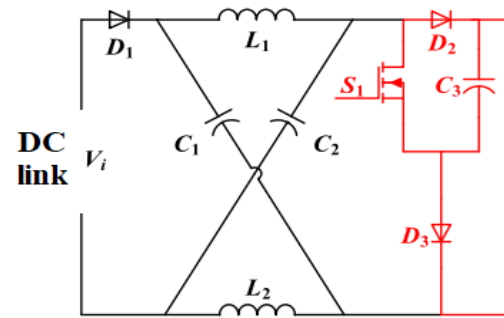


Figure 4: SZSC circuit structure

In the given circuit structure, the diode D1 is used to avoid reverse current flow to the renewable module [14]. The proposed SZSC has a very high voltage gain for very small duty ratio (D) of the switch S1. The output voltage of the SZSC is expressed as:

$$V_o = 1/((1-4D)) V_i \quad (7)$$

With this high gain a large range of voltages can be accessed with variable D value as per the requirement.

The proposed SZSC has the capability to operate in both continuous (CCM) and discontinuous conduction (DCM) modes. In DCM mode the inductor current reaches to zero for every switching cycle of the switch and in CCM mode the current doesn't touch zero [15]. As per the switching of S1 the converter operates in two states with each state having a different current cycle.

##### State 1: When S1 is ON

During this state the switch S1 is turned ON charging the passive elements L1 and L2 through D3 by Vi (generated by renewable module) [16]. The output capacitor C3 is considered to be in charged initially making the diode D2 to be in reverse biased condition. The C3 capacitor provides voltage to the MLI for conversion of DC to AC during this state. The current conduction path is given in figure 5 for state 1.

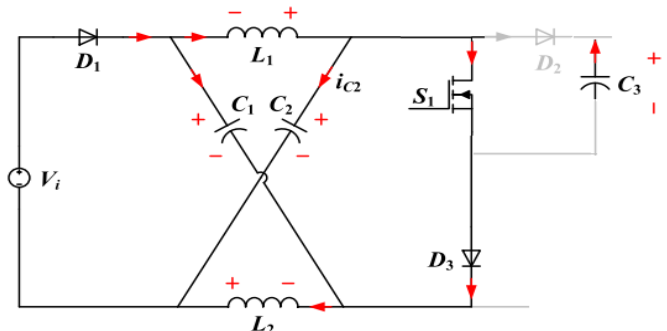


Figure 5: State 1 operating current conduction path

The capacitor C1 and C2 reduces voltage stress on L1 L2 and mitigating voltage spikes in these elements helps to improve their reliability [17]. The currents and voltages are expressed as:



$$i_{S1} = i_{L1} + i_{L2} \quad (8)$$

$$V_{L1} = V_{C1}; V_{L2} = V_{C2} \quad (9)$$

**State 2: When S1 is OFF**

At this state the switch S1 is turned OFF with the inductors L1 and L2 release their charge in series with the input voltage. As the capacitor C3 is discharge in previous state, in state 2 C3 charges through D3 with the combined voltages of Vi, VL1 and VL2. The current conduction path during state 2 is shown in figure 6.

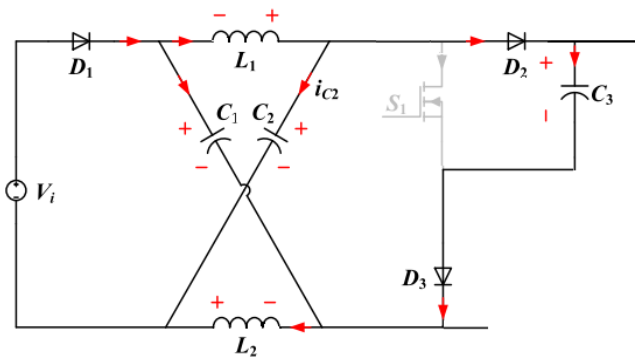


**Figure 6:** State 2 operating current conduction path

As the voltage of C3 is now less than the input voltage the diode D2 goes into forward bias condition providing voltage to the MLI. The voltages and currents of the elements are expressed as:

$$V_{C3} = V_o = V_{in} + V_{L1} + V_{L2} \quad (10)$$

$$i_{D1} = i_{L1} - i_{C1} ;$$

$$i_{D2} = i_{L1} + i_{C2} ;$$

$$i_{C3} = i_o - i_{D3} \quad (11)$$

Here  $i_o$  is the output current of SZSC. As per equation (6) the voltage developed at the output of SZSC depends on duty ratio of the switch S1 [18]. With higher duty ratio D, higher charge stored in L1 and L2 increases the output voltage during discharge. The parameters of the passive elements of the SZSC are calculated by the below expression:

$$L_1 = L_2 = \frac{2V_i D(1-D)}{\% \Delta I_L i_o f_s} \quad (12)$$

$$C_1 = C_2 = \frac{i_o D}{\% \Delta V_C V_i (1-2D)} \quad (13)$$

Here,  $\% \Delta I_L$  and  $\% \Delta V_C$  are the % current ripple and % voltage ripple tolerated by the inductor and capacitor respectively. ' $f_s$ ' is the switching frequency of the switch S1.

**3.3 Switched Capacitor MLI**

MLI are considered to be an optimal solution for interconnecting renewable sources to the grid. As most of the renewable sources are static sources the power generated by the sources are in DC voltage. To replicate a PWM AC voltage as Sin AC voltage, MLI concept is invented. The MLI creates staircase shaped voltage waveforms with increasing voltage levels decreasing the total harmonic distortion (THD) [19]. With increased number of voltage levels, the size of the LC filter reduces, decreasing the size and economy of the inverter. The proposed switched capacitor MLI has the capability to create multi-level AC voltage and also with increased magnitude [20]. The switched capacitor MLI circuit integrated to the SZSC fed renewable source is shown in figure 7.

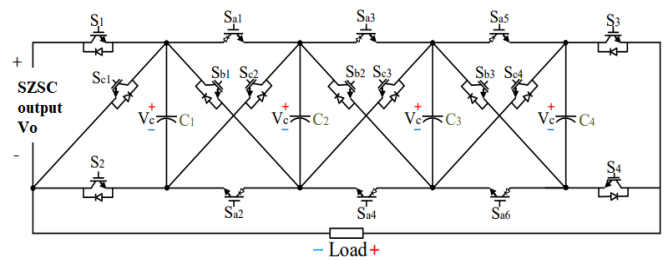


**Figure 7:** Switched capacitor MLI circuit structure

The proposed MLI has 9-levels of voltages with 4 on the positive side, 4 on negative side and zero is considered to be one level [21]. There are 11 body diode included n-p-n IGBTs (S1-S4, Sb1-Sb3, Sc1-Sc4), 6 only n-p-n IGBTs (Sa1-Sa6) and 4 capacitors (C1-C4). Different switching states of the IGBTs create four positive and four negative stair voltage levels. The switching states to the switched capacitor MLI switches are created by positive biased Sin waveform comparison to four level shifted triangular waveforms [22]. The gate pulses generation with the reference and carrier waveforms can be observed in figure 8.

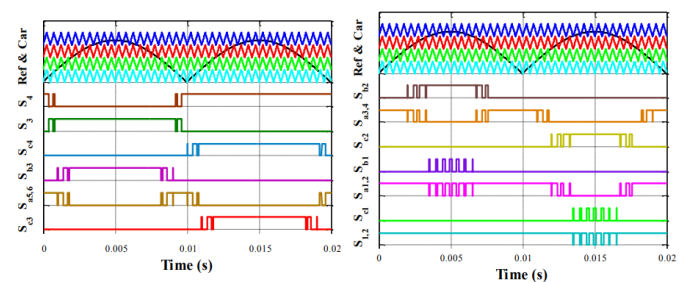


**Figure 8:** Gate pulses for the IGBT switches of MLI

The capacitors C1-C4 charge (C) and discharge (D) as per the switching cycle provided by figure 7 gate pulse generation [23]. The voltage levels and capacitor C and D are with respect to the switching states of the IGBTs is represented in table 1.

**Table 1: Voltage levels and capacitor states as per switching cycle**

Turned ON switches	C1	C2	C3	C4	Vout
Sb1, Sb2, Sb3, S1, S2, S3	C	D	D	D	4Vdc
Sa1, Sa2, Sb2, Sb3, S1, S2, S3	C	C	D	D	3Vdc
Sa1, Sa2, Sa3, Sa4, Sb3, S1, S2, S3	C	C	C	D	2Vdc
Sa1, Sa2, Sa3, Sa4, Sa5, Sa6, S1, S2, S3	C	C	C	C	Vdc
Sa1, Sa2, Sa3, Sa4, Sa5, Sa6, S1, S2, S4	C	C	C	C	0
Sa1, Sa2, Sa3, Sa4, Sc4, S1, S2, S4	C	C	C	D	-Vdc
Sa1, Sa2, Sc3, Sc4, S1, S2, S4	C	C	D	D	-2Vdc
Sc2, Sc3, Sc4, S1, S2, S4	C	D	D	D	-3Vdc
Sc1, Sc2, Sc3, Sc4, S4	D	D	D	D	-4Vdc

The capacitors C1-C4 provide voltages for a small instant of time creating voltage levels on the output side [24]. These capacitors are charged later during free-wheeling operating. For better voltage stability capacitors can be considered in the range of 1-5mF.

As per the switching *table 1* the modes of operation of the proposed MLI are shown in *figure 9a to 9h*.

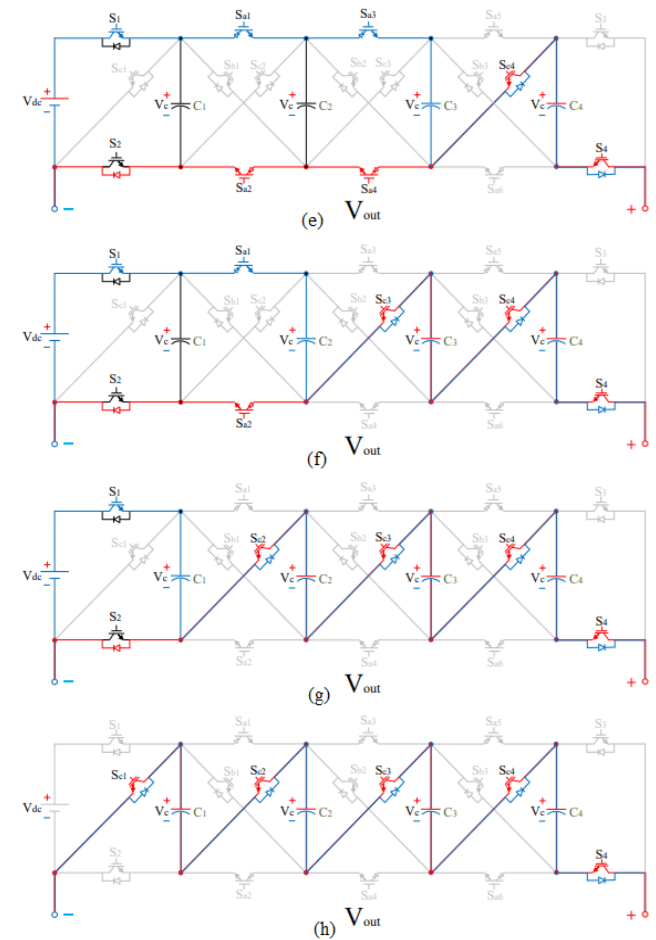
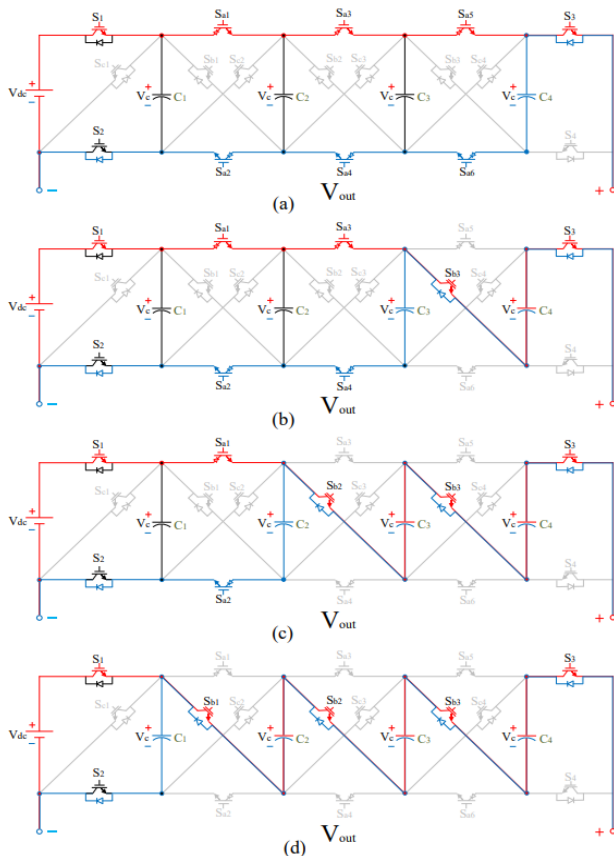


**Figure 9:** (a)  $V_o = V_{dc}$  (b)  $V_o = 2V_{dc}$  (c)  $V_o = 3V_{dc}$  (d)  $V_o = 4V_{dc}$  (e)  $V_o = -V_{dc}$  (f)  $V_o = -2V_{dc}$  (g)  $V_o = -3V_{dc}$  (h)  $V_o = -4V_{dc}$

The *figures 9(a) – (d)* are the switching patterns for positive levels generation  $V_{dc}$  to  $4V_{dc}$ . At the initial mode the capacitors C1 – C4 are charged with the input voltage. For every consecutive mode these capacitors come in series with the input voltage. The positive output voltage levels are expressed as:

$$V_o = V_{in} \text{ (level 1); } V_o = V_{in} + V_{c4} \text{ (level 2); } V_o = V_{in} + V_{c4} + V_{c3} \text{ (level 3); } V_o = V_{in} + V_{c4} + V_{c3} + V_{c2}$$

For the negative direction voltages with the updated switching pattern as per *table 1* the negative output voltage levels are expressed as:

$$V_o = -V_{c4} \text{ (level 1); } V_o = -V_{c4} - V_{c3} \text{ (level 2); } V_o = -V_{c4} - V_{c3} - V_{c2} \text{ (level 3); } V_o = -V_{c4} - V_{c3} - V_{c2} - V_{c1}$$

As per the switching pattern and the current conditions paths the nine level voltages are created. For PWM voltage generation the *figure 8* modulation technique is used providing gate pulses to the switches of the MLI.

#### 4. SIMULATION RESULTS

The modeling of the proposed test system with renewable sources and battery module connected SZSC MLI is done in MATLAB Simulink software. The blocks from 'Powersystems' were considered for the modeling and for THD analysis FFT (Fast Fourier Transformation) analysis tool is used. The graphs of different parameters are plotted for variable operating conditions created by changing solar irradiation ( $I_r$ ) and wind speed ( $V_w$ ) at specific time intervals. The performance of the SZSC and MLI are validated with these conditions of the renewable sources. The power balancing table is also given determining the efficiency of the converters. *Table 2* includes the system parameters for updating of the model with the given values.

**Table 2: Configuration parameters**

Name of the module	Parameters
PV unit	PVA: $V_{mp} = 13.5V$ , $I_{mp} = 5.65A$ , $V_{oc} = 16.2V$ , $I_{sc} = 6.02A$ , $N_s = 1$ , $N_p = 10$ , $P_{pv} = 762W$ . Boost converter: $L_b = 1mH$ , $C_{in} = 100\mu F$ , $R_{igt} = 1m\Omega$ , $f_s = 5kHz$ .
Wind farm unit	PMSG: $6Nm$ $300Vdc$ $4500rpm$ , $R_s = 0.62\Omega$ , $L_s = 2.075mH$ , $\phi = 0.08627V.s$ Buck-Boost converter: $L_{bbc} = 100\mu H$ , $R_{igt} = 1m\Omega$ , $f_s = 5kHz$ .
Battery unit	Battery: $V_{nom} = 12V$ , Capacity = 45Ahr. Bidirectional Converter: $L_{bdc} = 161.95\mu H$ , $C_{out} = 12mF$ , $R_{igt} = 1m\Omega$ , $f_s = 5kHz$ .
SZSC	$L1 = L2 = 360\mu H$ , $C1 = C2 = C3 = 330\mu F$ , $R_{mosfet} = 0.1\Omega$ , $C_{dc} = 1200\mu F$ , $V_{dc\ ref} = 100V$ , $K_p = 0.05$ , $K_i = 0.0035$ , $f_s = 5kHz$ .
MLI	$V_{in} = 100V_{dc}$ , $V_{out} = 240V_{ac\ rms}$ , $f_s = 2kHz$ , $R_{igt} = 1m\Omega$ , $C1 = C2 = C3 = C4 = 1mF$ .
Grid	$400V_{rms\ ph-ph}$ $50Hz$
Load	$500W$ $400V_{rms\ ph-ph}$ $50Hz$

The simulation of the test system with the parameters given in *table 2* are included and run for 3s with different operating settings. In order to validate the performance of the system, solar irradiation of the PV module and wind speed of the wind module are changed at specific intervals of time. The irradiation is changed from  $1000W/mt^2$  to  $500W/mt^2$  at 1s and wind speed is varied from 12m/s to 8m/s at 2s of simulation time. Graphs of measurements taken from the powers and voltages of the modules are recorded and plotted vs time. All the plotted graphs are generated by 'powergui' tool of the Simulink presented below.

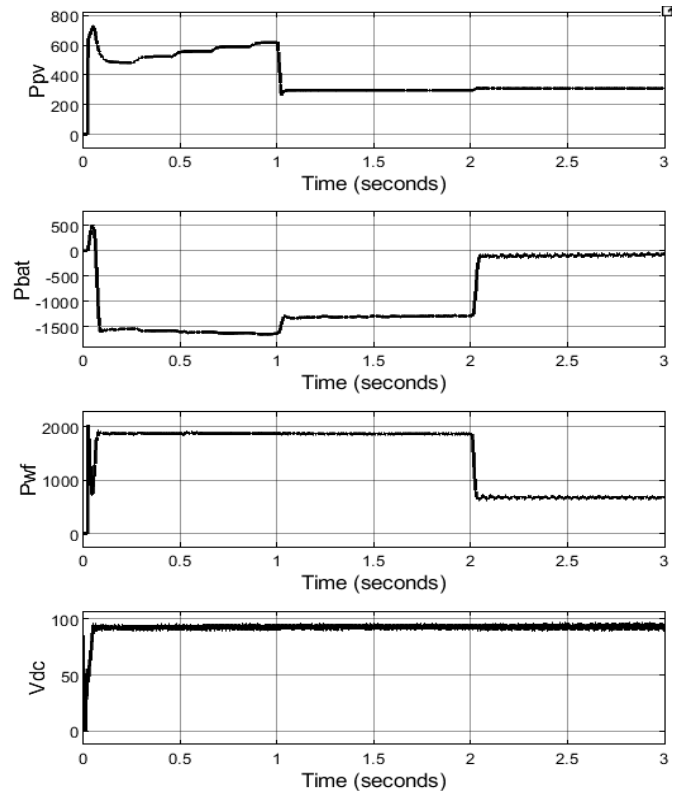


**Figure 10: Active powers of sources and DC link voltage**

In *figure 10* the active powers of the sources on the input side of the SZSC are presented. During 0-1s the PV module delivers 600W and wind farm unit generates 1800W. The total renewable power generated is 2400W, in which 800W is delivered to AC side through the SZSC and MLI. The remaining unutilized power of 1600W is stored in battery pack for utilization during deficit conditions. The PV module power is dropped to 300W at 1s and wind farm unit power is dropped to 600W at 2s as per the dynamic conditions created in the simulation. As per the change in the renewable powers the battery pack power storage varies accordingly. However, the power delivered to the inverter remains same at 800W in any given condition of irradiation and wind speed.

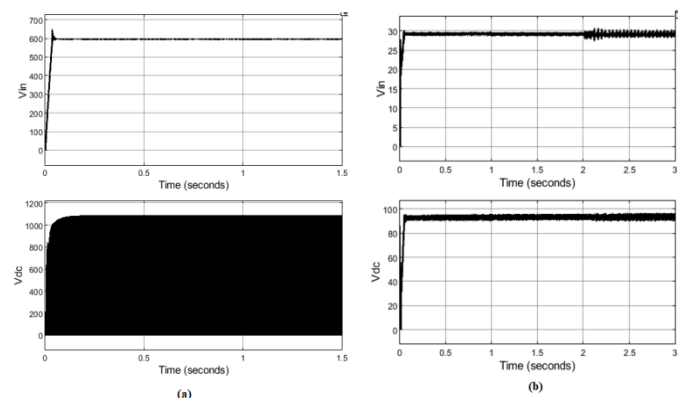


**Figure 11: Input and output voltages of (a) QZS (b) SZSC**

As observed in *figure 11a* the input voltage is at 600V which is boosted to 1100V for the inverter to generate 440 Vrms AC voltage. Whereas in *figure 11b* the input voltage to the SZSC is maintained stable at 30V for any changes in the operating conditions of renewable sources. The SZSC MLI topology can operate at input voltage level as low as 30V which is suitable for low rating renewable sources. This DC input voltage ( $V_{in}$ ) is stabilized by the CV controller of the battery module. The  $V_{in}$  is boosted to 95V by the SZSC circuit operated by voltage controller set with required reference output value. The input power to the SZSC ( $P_{in}$ ), output power of MLI ( $P_{out}$ ) and total power loss ( $P_{loss}$ ) of the circuits are presented in *figure 12*.

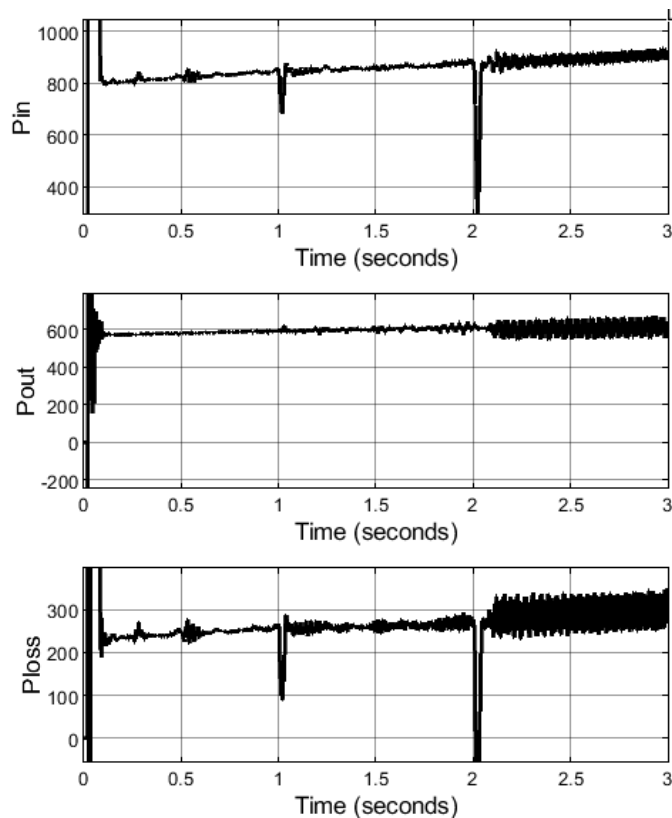


**Figure 12:** Input, Output and loss of power

As per the  $P_{in}$  graph it is validated that the power delivered to the SZSC is 800W-900W and the  $P_{out}$  is maintained at 600W. The  $P_{loss}$  is however is between 200W-300W varying as per the conditions on the source side.

From the powers of input and output of the converters in the system, the efficiency of the converter is calculated as:

$$\begin{aligned} \text{Efficiency} &= \frac{P_{out}}{P_{in}} \times 100 \\ &= \frac{450}{600} \times 100 = 75\% \end{aligned} \quad (14)$$

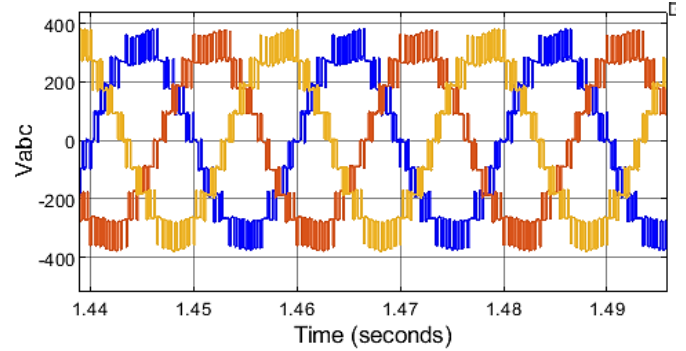


**Figure 13:** Multi-level inverter output voltage

*Figure 13* represents the multi-level voltage output of the proposed switched capacitor MLI with 9 voltage levels generated for reduction of harmonics on the grid side. The *figure 14* has the graphs of power supplied by renewable sources ( $P_{res}$ ), Power of the grid ( $P_{grid}$ ) and load demand power ( $P_{load}$ ).

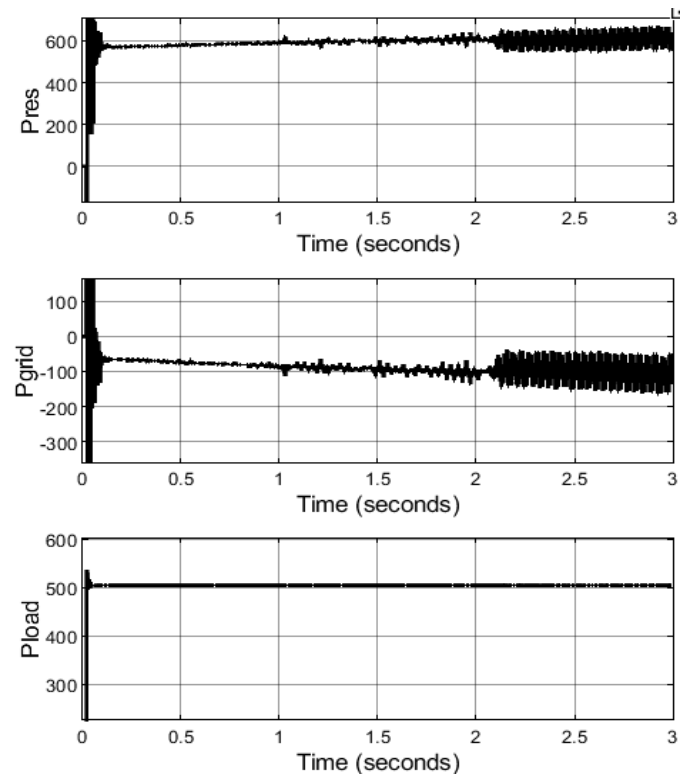


**Figure 14:** Renewable module, Grid and load active powers

As per *figure 14*, the power  $P_{res}$  delivered to the AC side through the SZSC MLI is 600W,  $P_{load}$  demand is 500W and the power excess power of 100W from renewable source side is injected to grid. The negative power of  $P_{grid}$  in the graph represents injection of power to the grid. A harmonic analysis is carried out on the load voltage using FFT analysis tool to determine the THD of the waveform.



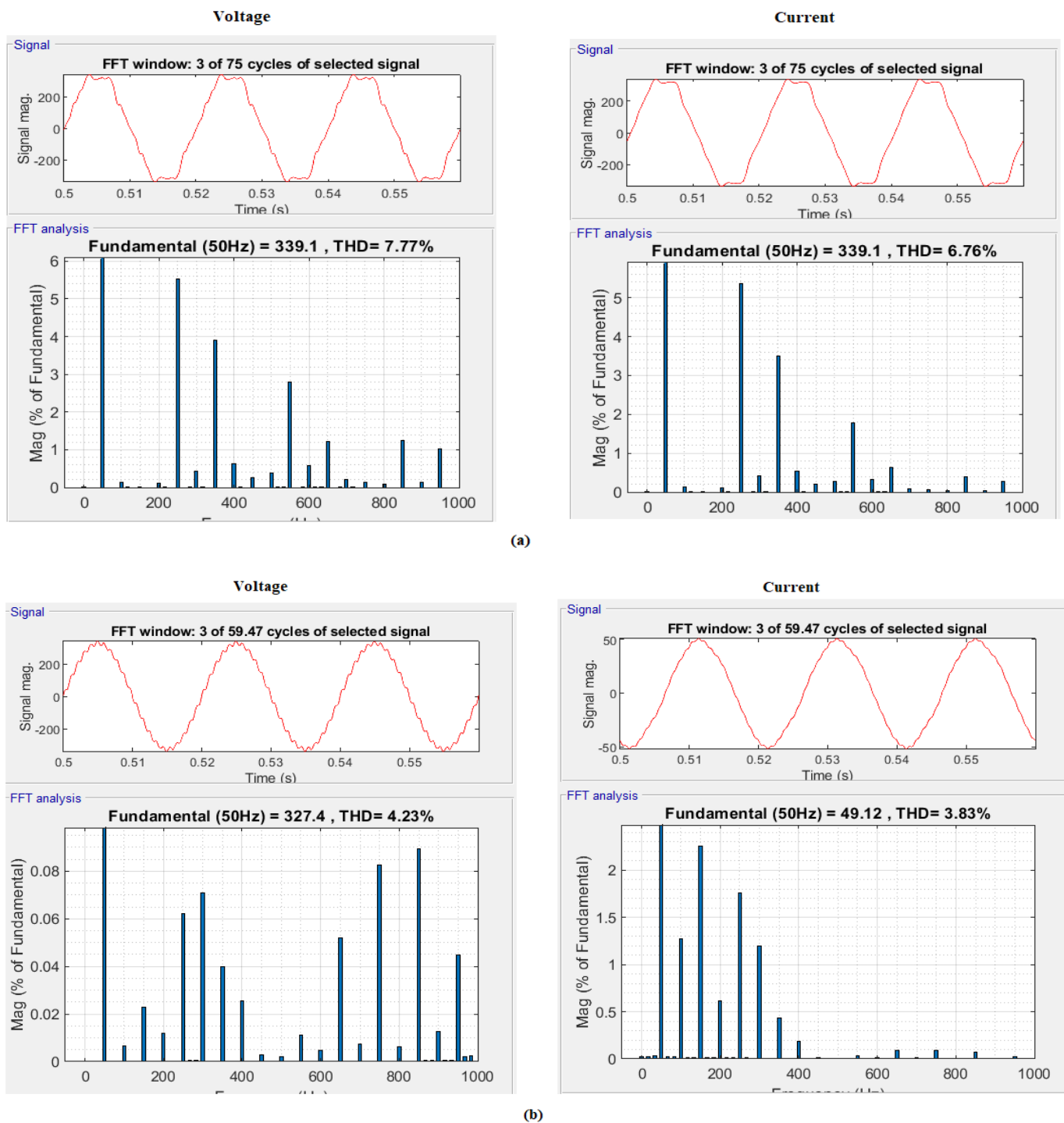


**Figure 15:** THD of load voltage(a) QZS (b)SZSC

The THD of the load voltage analyzed when the system is stable is shown in *figure 15a* and *15b* with QZS and SZSC topologies respectively. The analysis indicates that the THD of the inverter voltage is maintained at 7.77% and 4.23%, THD of inverter current is maintained at 6.76% and 3.83% for QZS and SZSC MLI respectively. The SZSC MLI has lower THD as compared to the QZS system validating the performance of the SZSC MLI topology. As per IEEE Std 519-2022 the harmonics are maintained below 5% making it a stable system.

## 5. CONCLUSION

The low voltage renewable sources are inter-connected to grid sharing power to the load integrated with high voltage gain capability SZSC switched capacitor MLI. The DC link voltage with magnitude of 30V feeding from PV source, wind farm unit and battery module is successfully converted to 3-ph 415V AC voltages. The DC link voltages at the input and output of the SZSC are stabilized by individual CV controllers with specific reference values. The SZSC creates nearly

3times gain DC voltage of 95V which is further converted to multi-level 3-ph AC voltages by the switched capacitor MLI. The complete system is stable with very low ripple in the DC input and output voltages even during variable conditions of the renewable sources. The current THD is recorded at 6.76% and 3.83% for QZS and SZSC MLI respectively calculated using FFT analysis tool available in 'powergui' toolbox. The THD is same for both load voltage and current. Comparatively the THD of the SZSC MLI is lower than QZS topology. The renewable power is shared to the grid and load on the AC side also charging the battery pack through the bidirectional converter on the DC side. The system delivers 600W of renewable power to the grid with an efficiency of 75% out of 800W. The proposed topology has high gain capability, low harmonic content and moderate efficiency as compared to many traditional methods of renewable source interconnection to grid.

## REFERENCES

[1] Bharatee, A.; Ray, P.K.; Subudhi, B.; Ghosh, A. "Power Management Strategies in a Hybrid Energy Storage System Integrated AC/DC Microgrid", A Review. *Energies* 2022, 15, 7176. <https://doi.org/10.3390/en15197176>

[2] F. Nejabatkhah and Y. W. Li, "Overview of Power Management Strategies of Hybrid AC/DC Microgrid," in *IEEE Transactions on Power Electronics*, vol. 30, no. 12, pp. 7072-7089, Dec. 2015, doi: 10.1109/TPEL.2014.2384999.

[3] J. Liu, J. Wu, J. Qiu and J. Zeng, "Switched Z-Source/Quasi-Z-Source DC-DC Converters With Reduced Passive Components for Photovoltaic Systems," in *IEEE Access*, vol. 7, pp. 40893-40903, 2019, doi: 10.1109/ACCESS.2019.2907300.

[4] N. Javaid et al., "An intelligent load management system with renewable energy integration for smart homes," *IEEE Access*, vol. 5, pp. 13587-13600, 2017.

[5] G. Zhang, B. Zhang, Z. Li, D. Qiu, L. Yang, and W. A. Halang, "A 3-Z-network boost converter," *IEEE Trans. Ind. Electron.*, vol. 62, no. 1, pp. 278-288, Jan. 2015.

[6] Kumar, R.; Kannan, R.; Nor, N.B.M.; Mahmud, A. A High Step-Up Switched Z-Source Converter (HS-SZC) with Minimal Components Count for Enhancing Voltage Gain. *Electronics* 2021, 10, 924. <https://doi.org/10.3390/electronics10080924>

[7] M. Samizadeh, X. Yang, B. Karami, W. Chen, F. Blaabjerg and M. Kamranian, "A New Topology of Switched-Capacitor Multilevel Inverter With Eliminating Leakage Current," in *IEEE Access*, vol. 8, pp. 76951-76965, 2020, doi: 10.1109/ACCESS.2020.2983654.

[8] León Gómez, J.C.; De León Aldaco, S.E.; Aguayo Alquicira, J. A Review of Hybrid Renewable Energy Systems: Architectures, Battery Systems, and Optimization Techniques. *Eng* 2023, 4, 1446-1467. <https://doi.org/10.3390/eng4020084>

[9] A. F. Tazay, A. M. A. Ibrahim, O. Noureldeen and I. Hamdan, "Modeling, Control, and Performance Evaluation of Grid-Tied Hybrid PV/Wind Power Generation System: Case Study of Gabel El-Zeit Region, Egypt," in *IEEE Access*, vol. 8, pp. 96528-96542, 2020, doi: 10.1109/ACCESS.2020.2993919.

[10] M. M. Gulzar, A. Iqbal, D. Sibtain and M. Khalid, "An Innovative Converterless Solar PV Control Strategy for a Grid Connected Hybrid PV/Wind/Fuel-Cell System Coupled With Battery Energy Storage," in *IEEE Access*, vol. 11, pp. 23245-23259, 2023, doi: 10.1109/ACCESS.2023.3252891.

[11] M. Ghofrani and N. N. Hosseini, "Optimizing Hybrid Renewable Energy Systems": A Review, *Sustainable Energy - Technological Issues, Applications and Case Studies. InTech*, Dec. 21, 2016. doi: 10.5772/65971.

[12] A. A. Z. Diab, H. M. Sultan, I. S. Mohamed, O. N. Kuznetsov and T. D. Do, "Application of Different Optimization Algorithms for Optimal Sizing of PV/Wind/Diesel/Battery Storage Stand-Alone Hybrid Microgrid," in *IEEE Access*, vol. 7, pp. 119223-119245, 2019, doi: 10.1109/ACCESS.2019.2936656.

[13] S. Rostami, V. Abbasi and M. Parastesh, "Design and Implementation of a Multiport Converter Using Z-Source Converter," in *IEEE Transactions on Industrial Electronics*, vol. 68, no. 10, pp. 9731-9741, Oct. 2021, doi: 10.1109/TIE.2020.3022538.

[14] A. Kumar, Y. Wang, M. Raghuram, P. Naresh, X. Pan and X. Xiong, "An Ultra High Gain Quasi Z-Source Inverter Consisting Active Switched Network," in *IEEE Transactions on Circuits and Systems II: Express Briefs*, vol. 67, no. 12, pp. 3207-3211, Dec. 2020, doi: 10.1109/TCSII.2020.2970723.

[15] H. -K. Yang and J. -W. Park, "Sawtooth-Carrier-Based Pulsewidth Modulation Method for Quasi-Z-Source Inverter With Zero-Voltage-Switching Operation to Reduce Harmonic Distortion and Inductor Current Ripple," in *IEEE Transactions on Industrial Electronics*, vol. 68, no. 2, pp. 916-924, Feb. 2021, doi: 10.1109/TIE.2020.2967710.

[16] Qixiang Huang, Feng Wang & Jamal Abbasi Bolaghi (2023), "Improved Switched-Capacitor Switched-Inductor Z-source Inverter for Increasing Boost Factor and Decreasing Voltage Capacitors Stress," *IETE Journal of Research*, 69:6, 3887-3896, DOI: 10.1080/03772063.2021.1923077

[17] Yuan, J.; Yang, Y.; Blaabjerg, F. "A Switched Quasi-Z-Source Inverter with Continuous Input Currents," *Energies* 2020, 13, 1390. <https://doi.org/10.3390/en13061390>

[18] Y. Zhang, Q. Liu, Y. Gao, J. Li and M. Sumner, "Hybrid Switched-Capacitor/Switched-Quasi-Z-Source Bidirectional DC-DC Converter With a Wide Voltage Gain Range for Hybrid Energy Sources EVs," in *IEEE Transactions on Industrial Electronics*, vol. 66, no. 4, pp. 2680-2690, April 2019, doi: 10.1109/TIE.2018.2850020.

[19] R. Barzegarkhoo, M. Forouzes, S. S. Lee, F. Blaabjerg and Y. P. Siwakoti, "Switched-Capacitor Multilevel Inverters: A Comprehensive Review," in *IEEE Transactions on Power Electronics*, vol. 37, no. 9, pp. 11209-11243, Sept. 2022, doi: 10.1109/TPEL.2022.3164508.

[20] Deng, Z.; Zhu, X.; Duan, J.; Ye, J.; Wang, Y. "A Multilevel Switched Capacitor Inverter with Reduced Components and Self-Balance". *Appl. Sci.* 2023, 13, 8955. <https://doi.org/10.3390/app13158955>

[21] Md N.H. Khan, R. Barzegarkhoo, Y.P. Siwakoti, S.A. Khan, L. Li, F. Blaabjerg, "A new switched-capacitor multilevel inverter with soft start and quasi resonant charging capabilities," *International Journal of Electrical Power & Energy Systems*, Volume 135, 2022, 107412, ISSN 0142-0615, <https://doi.org/10.1016/j.ijepes.2021.107412>.

[22] Kasinath Jena, Dhananjay Kumar, B. Hemanth Kumar, K. Janardhan, Arvind R. Singh, Raj Naidoo, Ramesh C. Bansal, "A Single DC Source Generalized Switched Capacitors Multilevel Inverter with Minimal Component Count," *International Transactions on Electrical Energy Systems*, vol. 2023, Article ID 3945160, 12 pages, 2023. <https://doi.org/10.1155/2023/3945160>

[23] Wang, Y., Ye, J., Ku, R. et al. "A modular switched-capacitor multilevel inverter featuring voltage gain ability," *J. Power Electron.* 23, 11-22 (2023). <https://doi.org/10.1007/s43236-022-00508-9>

[24] Tapas Roy, Sitakant Debata & Pradip Kumar Sadhu (2023), "A high boost switched capacitor multilevel inverter with reduced components," *International Journal of Electronics*, DOI: 10.1080/00207217.2023.2248664.



© 2024 by the Sapavath Sreenu1, Dr. J Upendar. Submitted for possible open access publication under the terms and conditions of the Creative Commons Attribution (CC BY) license (<http://creativecommons.org/licenses/by/4.0/>).